



## Research article

# Construction and validation of a novel prognostic signature for cutaneous melanoma based on ferroptosis-related genes

Wenna Guo<sup>a,b</sup>, Xue Wang<sup>a</sup>, Yanting Zhang<sup>a</sup>, Hongtao Liu<sup>a</sup>, Shanshan Ma<sup>a,\*\*</sup>, Fangxia Guan<sup>a,\*</sup>

<sup>a</sup> School of Life Sciences, Zhengzhou University, Zhengzhou, 450001, China

<sup>b</sup> School of Basic Medical Sciences, Zhengzhou University, Zhengzhou, China



## ARTICLE INFO

## Keywords:

Cutaneous melanoma  
Prognosis  
Ferroptosis  
Risk stratification  
Immune infiltration

## ABSTRACT

Ferroptosis, a recently uncovered iron-dependent, non-apoptotic cell death process, has been increasingly linked to cancer development. In this study, our objective was to develop a prognostic model centered on ferroptosis-related genes (FRGs) and assess its efficacy as an overall survival (OS) prediction biomarker. We conducted a systematic analysis of cutaneous melanoma (CM) and devised a novel ferroptosis-related prognostic signature (FRGSig) using the TCGA database. An independent dataset from GSE65904 was employed to corroborate the validity of the FRGSig. Both univariate and multivariate Cox proportional hazard regression analyses were utilized to construct a FRGSig composed of five FRGs. mRNA expression and immunohistochemistry (IHC) analysis demonstrated that the expression of FRGSig genes varied between tumor and normal tissues. According to Kaplan-Meier analysis, patients with elevated FRGSig scores faced a worse prognosis. The predictive accuracy of FRGSig was evaluated using the time-dependent receiver operating characteristic curve (ROC), with the area under the curve (AUC) values for 1, 3, and 5 OS at 0.682, 0.711, 0.735 in the TCGA cohort, and 0.662, 0.695, 0.712 in the validation dataset, respectively. Univariate and multivariate Cox regression analyses demonstrated that FRGSig served as an independent prognostic factor. Further analysis revealed a significant relationship between FRGSig and Tumor Mutational Burden (TMB) as well as immune infiltration levels. Gene set enrichment analysis (GSEA) disclosed functional disparities between high- and low-risk groups, suggesting that immune checkpoint-related pathways could be instrumental in the improved prognosis of the low-risk group. Taken together, the FRGSig has potential guidance for prognosis prediction and clinical treatment of CM.

**Abbreviations:** CM, Cutaneous melanoma; TCGA, The Cancer Genome Atlas; GEO, Gene Expression Omnibus; GEPIA, Gene Expression Profiling Interactive Analysis; ROC, Receiver operating characteristic; AUC, Area under the receiver operating characteristic curve; OS, Overall survival; HR, Hazard Ratio; CI, Confidence interval; FRG, Ferroptosis-related gene; FRGSig, FRG signature; TMB, Tumor mutational burden; ICG, Immune checkpoint-related genes; ARNTL, Aryl hydrocarbon receptor nuclear translocator like; EGFR, Epidermal growth factor receptor; IFNG, Interferon gamma; NOX4, NADPH oxidase 4; TFAP2C, Transcription factor AP-2 gamma; IHC, Immunohistochemistry; GO, Gene Ontology; KEGG, Kyoto Encyclopedia of Genes and Genomes.

\* Corresponding author.

\*\* Corresponding author.

E-mail addresses: [mashanshan84@163.com](mailto:mashanshan84@163.com) (S. Ma), [fxguan@126.com](mailto:fxguan@126.com) (F. Guan).

<https://doi.org/10.1016/j.heliyon.2023.e15725>

Received 22 March 2022; Received in revised form 9 April 2023; Accepted 19 April 2023

Available online 24 April 2023

2405-8440/© 2023 Published by Elsevier Ltd.

This is an open access article under the CC BY-NC-ND license

(<http://creativecommons.org/licenses/by-nc-nd/4.0/>).

## 1. Background

Cutaneous melanoma (CM) is a highly aggressive cancer type originating from mutated melanocytes, characterized by high mutagenicity, early metastasis and elevated mortality [1,2]. Over the past 40 years, the incidence of CM has increased six-fold [3]. According to statistics, there were 4,106 new CM cases per 100,000 population in China in 2020 [4]. Due to the rapid progression and high genetic heterogeneity of CM, patients with CM generally have a poor prognosis [5,6]. This makes CM remain an enormous public health problem [7]. Prognostic assessment is a critical reference for the treatment and management of CM patients, and prognostic biomarkers enable reliable stratification of patients based on risk level [8]. In order to improve the benefit/risk ratio of individual patients, it is crucial to discover biomarkers that are capable of predicting the likelihood of treatment outcome. Therefore, developing new robust prognostic biomarkers of CM is urgently needed to improve patient survival.

Recently, tumor ferroptosis has caused widespread concern. Since Dixon proposed the concept of ferroptosis in 2012, accumulating evidence suggested that ferroptosis plays an influential function in regulating the occurrence, development and treatment of cancer by inducing tumor cells death and inhibiting tumor growth [9,10]. For example, lower expression of ferroptosis-related gene (FRG) MGST1 is associated with higher survival rate in lung cancer [11]. FRGs such as GPX4, SLC7A11 were found to be linked to temozolomide resistance in glioma [12]; miR-137 was found to regulate ferroptosis by targeting SLC1A5 in CM cells [13]. However, further investigation is needed to understand the prognostic promises and potential molecular mechanisms of FRGs in CM.

Herein, we built and verified a new prognostic biomarker for CM using FRGs. The relationship between FRGs and the prognostic value in CM was investigated, and a FRG signature (FRGSig) was identified as prognostic predictor on the basis of the TCGA CM cohort. The FRGSig was subsequently confirmed in validation cohort. The associations between FRGSig, clinicopathological features, tumor mutational burden (TMB) and immune infiltration levels was elucidated to further explore the potential of FRGSig as a clinical therapeutic target. Additionally, biological functions and pathways relating to the FRGSig were illustrated through functional enrichment analysis.

## 2. Materials and methods

### 2.1. Data collection and processing

The clinical data of CM patients were acquired from the TCGA database [14]. Gene expression profile of CM patients were also obtained from RNA-seq data in the TCGA database, and gene expression levels were defined and normalized as  $\log_2(\text{FPKM}+1)$ . Microarray datasets, including transcriptomic data and clinical data of CM patients were accessed from GSE65904 in the GEO database [15,16]. The mRNA expression of 461 CM tumor and 558 normal skin tissues were gained from GEPIA database. FRGs were gathered from the FerrDb database.

### 2.2. Development and evaluation of FRG prognostic signature (FRGSig)

Cox proportional hazards regression was applied to identify crucial gene related to patient survival [17]. Univariate analysis was used for determining the prognostic-related FRGs ( $P < 0.05$ ), while multivariate analysis was applied to search for prognostic factors, and calculate the regression coefficients of each gene. Afterwards, the FRGSig was constructed. The risk score (patients) =  $\sum$  regression coefficient (prognostic gene) \* expression (prognostic gene). Kaplan-Meier curve, widely used in clinical studies, was applied to measure and compare survival probabilities of CM patients [18]. Time-dependent ROC analysis evaluated the survival predictive capability of the FRGSig [19]. In addition, nomogram plots were built based on FRGSig and clinicopathological features.

### 2.3. Immunohistochemistry (IHC)

The IHC images of normal skin tissue and CM tissue were acquired from The Human Protein Atlas (HPA) database, which analyzed protein levels of genes. The criteria for antibodies were to be as specific as possible relative to all other protein-coding genes [20,21]. The primary antibodies used in HPA database used were as follows: anti-ARNTL (CAB045962); anti-EGFR (HPA001200); anti-IFNG (CAB010344); anti-TFAP2C (HPA055179).

### 2.4. Relationship between FRGSig and TMB, immune cell infiltration

Correlation analysis was performed to reveal the association between FRGSig and TMB. Given that tumor immune infiltration could be regulated by the immune checkpoints, the correlation between FRGSig and immune checkpoint-related genes (ICGs) were analyzed. The difference in expression of ICGs between patients in high- and low-risk groups were compared. Spearman's coefficient was applied to calculate correlations, and the Mann-Whitney  $U$  test was carried out to evaluate gene expression differences between the two groups.

### 2.5. Functional enrichment analysis

GO, KEGG and Reactome pathway enrichment analyses were performed using GSEA to identify functional categories and signal pathways associated with FRGSig [22]. Briefly, according to the median FRGSig risk score, patients were separated into high- ( $n_1 =$

228) and low-risk groups (n2 = 228). GSEA was used to seek signaling pathways involved between the two groups for the discovered genes. Gene sets with a nominal P value < 0.05 and |NES| > 1.5 were regarded as statistically significant.

2.6. Statistical analysis

Cox regression analyses were carried out using R package “survival” and “survminer”. Kaplan–Meier analysis and generalized Wilcoxon test were carried out using R package “survival” to visualize and calculate statistical differences in OS between the different risk groups. ROC analysis was conducted using R package “survivalROC” to determine the sensitivity and specificity of FRGSig in prognosis prediction. A nomogram composed of FRGSig and clinical factors was established using R package “rms”. The Mann–Whitney U test was carried out to evaluate the difference in gene expression between the two groups of non-normal distributed variables.

3. Results

3.1. Identification and evaluation of FRGSig in TCGA cohort

456 CM patients from TCGA database were investigated, including 286 males and 170 females. The age at diagnosis varied from 15 to 90 years, with a mean age of 58 years. The Breslow thickness was 0–75 mm, with a mean of 3.0 mm, and 6, 76, 136, 170, and 23 patients in stage 0, I, II, III, and IV, respectively. 348 FRGs were acquired from the FerrDb database, which included 167 ferroptosis driver genes, 104 ferroptosis suppressor genes and 113 ferroptosis marker genes. Univariate Cox regression analysis found 103 FRGs were significantly related to the prognosis of CM patients (P < 0.05). These 103 FRGs were chosen for further multivariate analysis to build prognostic model, and a FRGSig containing five genes (ARNTL, EGFR, IFNG, NOX4 and TFAP2C) was screened out based on the ROC analysis. The prognostic risk score = (−0.568 \* expression level of ARNTL) + (0.14 \* Exp<sub>EGFR</sub>) + (−0.339 \* Exp<sub>IFNG</sub>) + (−0.185 \* Exp<sub>NOX4</sub>) + (0.146 \* Exp<sub>TFAP2C</sub>), in which Exp refers to the expression level of gene. Fig. 1A and B showed the relationship between these five genes and the OS of patients. The information related to these five genes is shown in Table S1. For these five genes, the expression levels of ARNTL, IFNG, NOX4, TFAP2C were significantly increased in long-OS patients (>5 years), whereas the expression of EGFR was significantly decreased in short-OS patients (<5 years) (Fig. 2A) (P < 0.05).

Thereafter, we computed the risk scores for each CM patient on the basis of the prognostic signature. Then, patients were separated into high-risk group (n1 = 228) and low-risk group (n2 = 228) in accordance with the median risk dispersion (−1.223). Principal component analysis (PCA) indicated the continuous capturing of five FRGs (Fig. 2B), and a significant distribution difference between the two group patients (Fig. 2C). Kaplan–Meier survival curves demonstrated significant differences in OS of patients between the two group (Fig. 2D). The AUC for OS prediction was calculated to verify the predictive competence of FRGSig, and the AUC (95% CI) values

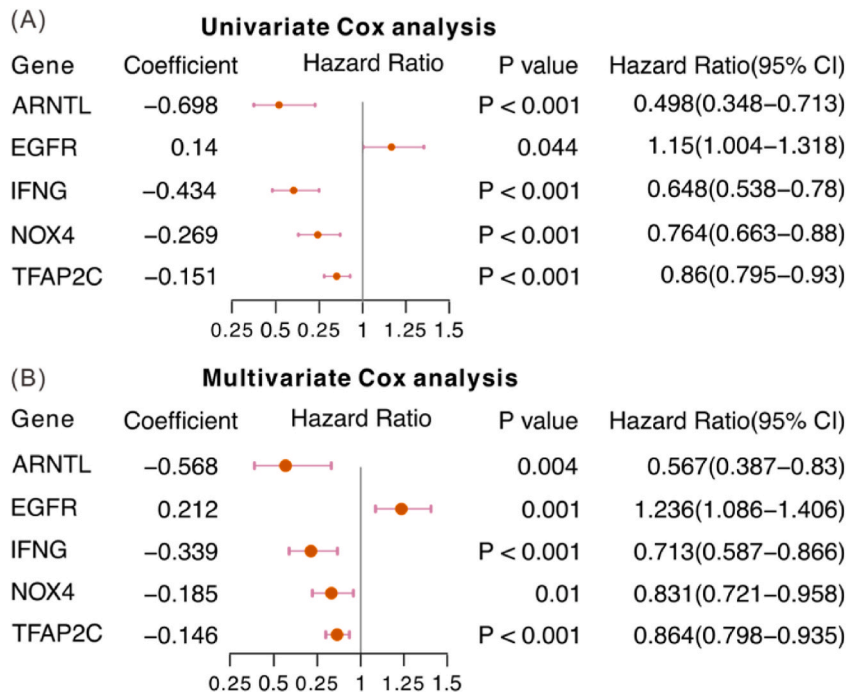
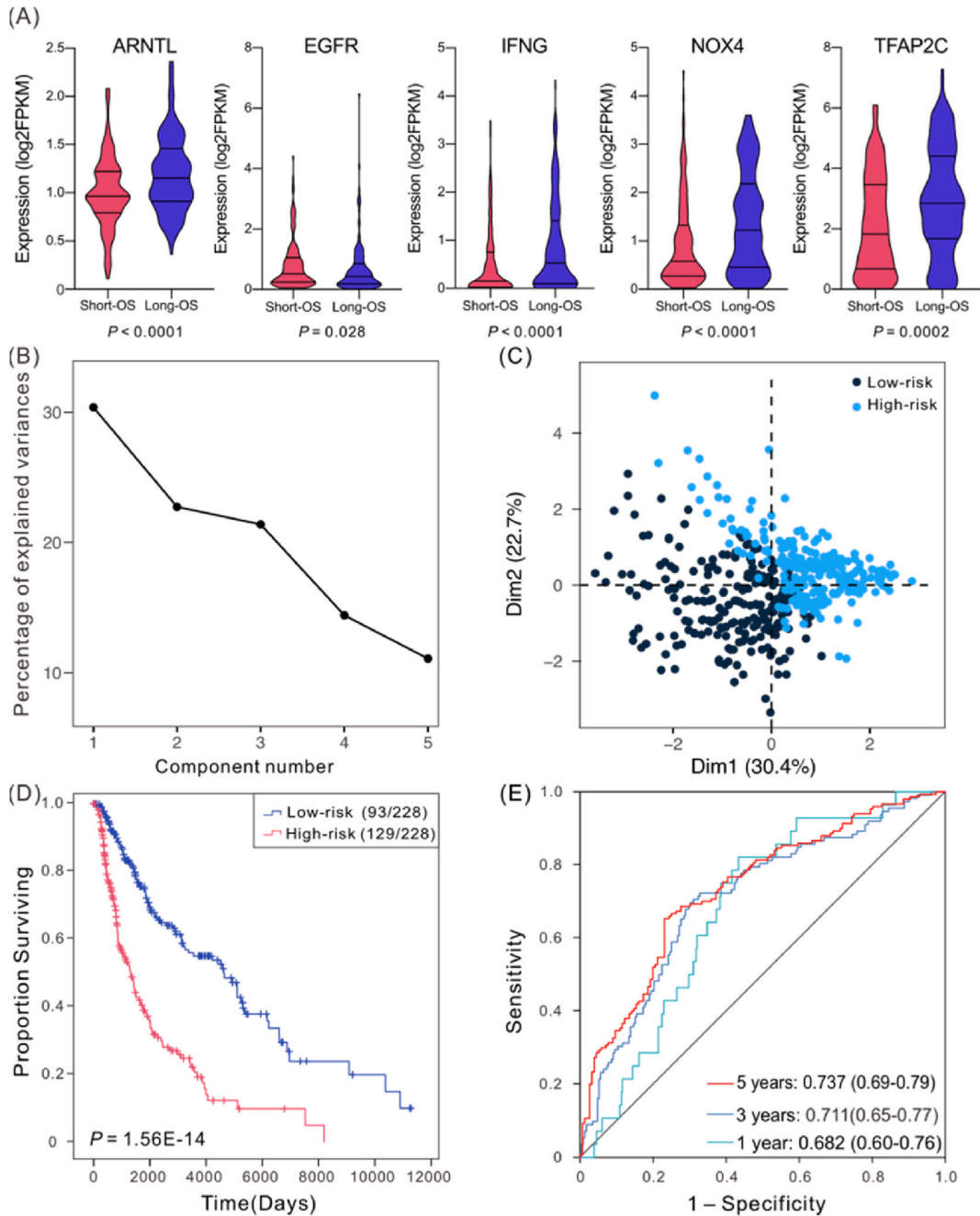


Fig. 1. The results of univariate and multivariate Cox regression analyses showed a significant correlation between gene expression and overall survival (OS).



**Fig. 2. Evaluation of the prognostic signature.** (A) The violin plots of gene expression levels in short-OS (<5 years) and long-OS patients (>5 years) in the TCGA cohort. (B) The Kaplan-Meier analysis was used to visualize the OS of patients in low- and high-risk groups, and the Wilcoxon test was applied to compare the difference. (C) The contributing components were ranked on the basis of the magnitude of the corresponding percentage of explained variance in the principal component analysis (PCA). (D) PCA plots of the high- and low-risk groups in TCGA cohort. (E) The AUC values for the 1, 3, and 5-year OS assessed the prognostic predictive accuracy of FRGSig in TCGA.

for 1-, 3-, and 5-year OS were 0.682 (0.59–0.76), 0.711 (0.65–0.77), 0.737 (0.69–0.79), respectively (Fig. 2E), indicating that the FRGSig presented good performance on prognosis prediction. Kaplan–Meier analysis of individual gene displayed a significant discrepancy in OS between patients with different gene expressions (Fig. S1). Furthermore, a nomogram was generated to provide patient survival information by univariate and multivariate analysis, the results indicated the nomogram model consisting of five genes was helpful in prognosis prediction (Fig. S2A). ROC analysis further showed that FRGSig had higher prediction accuracy than single gene (Fig. S2B).

### 3.2. Expression of FRGSig genes

To evaluate the expression level of these five genes in CM, we obtained the mRNA expression of normal skin tissue and CM tissue from GEPIA. We found that the mRNA expression levels of these five genes were remarkably distinct between tumor and normal tissues (Fig. S3). We also compared the protein expression levels of these genes in the HPA database. IHC displayed moderate staining for ARNTL and IFNG in CM tumor tissues (Fig. 3A, C), whereas EGFR and TFAP2C were negative in CM tumor tissues (Fig. 3B, D). Combined with the coefficients of the risk score formula, we hypothesized that these genes might have comprehensive effect on melanoma development and prognosis.

### 3.3. Validation of the FRGSig in independent GEO dataset

To test the stability of the FRGSig, we incorporated patients from the GEO database (GSE65904,  $n = 210$ ) into the predictive model for validation. As expected, patients with low risk scores showed a significant improvement in OS in comparison to patients with high risk scores ( $P < 0.01$ ) (Fig. 4A). ROC analysis indicated that AUCs (95% CI) for 1, 3, and 5-year OS were 0.662 (0.57–0.75), 0.695 (0.61–0.78), and 0.712 (0.61–0.82), respectively (Fig. 4B). These results supported that FRGSig was also effective in risk stratification in independent datasets.

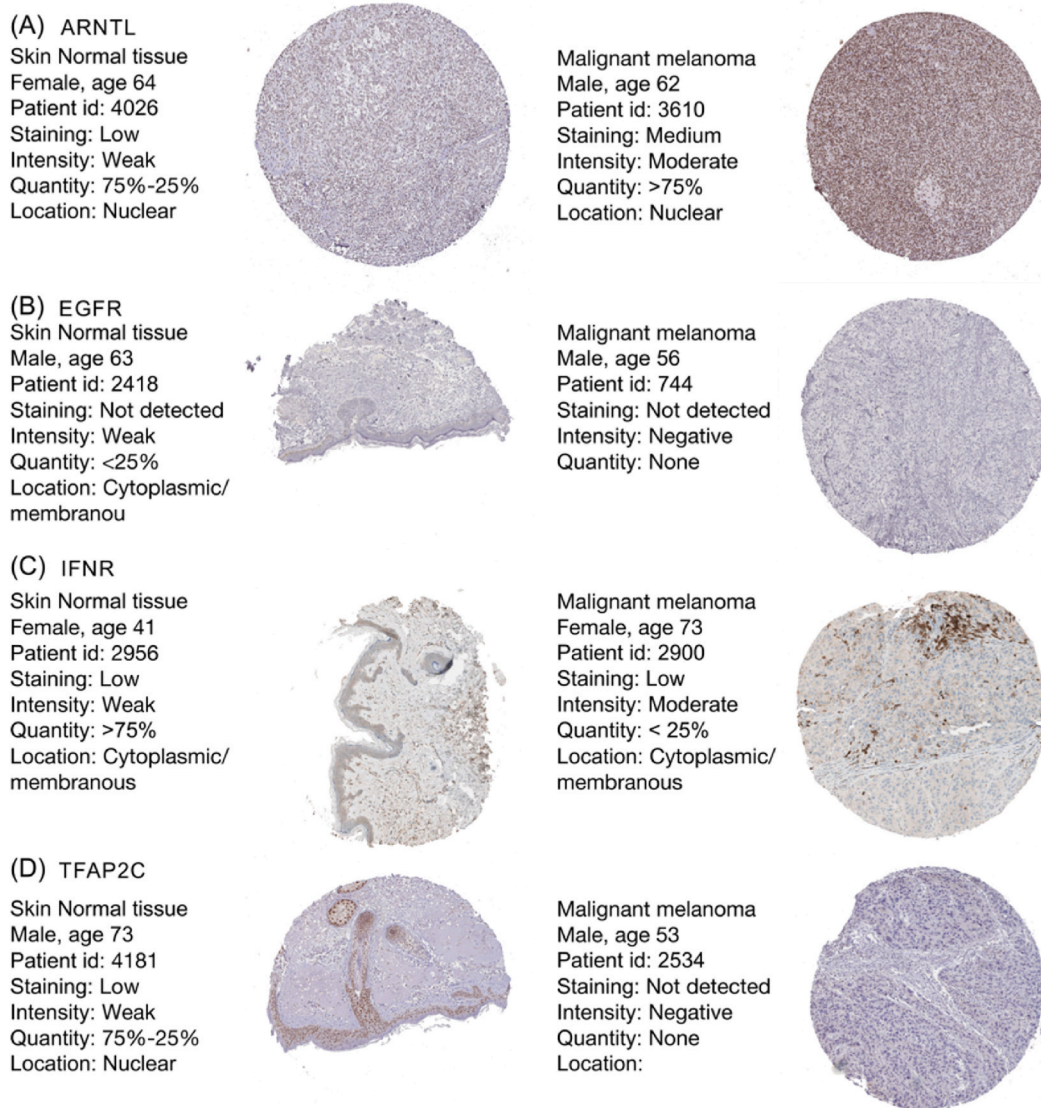


**Fig. 3.** Representative specimens exhibiting IHC labeling pattern of four genes in normal skin tissue and CM tissue are presented. (A) ARNTL. (B) EGFR. (C) IFNG (D) TFAP2C.

### 3.4. Independence of the FRGSig from other clinical features

Clinical parameters such as patients' age, stage, tumor thickness, as well as localization of the primary tumor or the presence of metastases can also affect the outcome of CM patients. We analyzed the FRGSig risk scores for primary and metastatic tissues, and found that the higher risk scores for primary tissues than for metastatic tissues (Fig. S4A). Kaplan–Meier survival analysis found that patients with primary tissues had significantly shorter OS than those with metastatic tissues (Fig. S4B), which was consistent with the FRGSig risk scores, indicating that our risk assessment was correct. To further explore the characteristics of FRGSig, an exploration analysis of the risk score and clinical parameters was carried out. Clinical features, such as age, gender, stage, breslow depth, were used along with the FRGSig risk score to establish the nomogram and estimate individualized risk scores. It was found that the FRGSig score was significantly correlated with OS in both univariate (HR 2.738, 95% CI: 2.123–3.531,  $P < 0.001$ ) (Fig. 5A) and multivariate Cox analyses (HR 2.883, 95% CI: 2.099–3.96,  $P < 0.001$ ) (Fig. 5B), indicating that the FRGSig may be considered as an independent marker. The nomogram demonstrated that the FRGSig had good accuracy, and was more reliable than clinicopathological variables in predicting OS of CM patients (Fig. 5C). These results confirmed that the FRGSig was an independent prognostic biomarker of CM patients.

To further confirm the applicability of FRGSig, we regrouped patients according to different clinicopathological characteristics. The results demonstrated that the FRGSig was effective in the identification of the high- and low-risk patients regardless of gender, age, stage and breslow depth grouping, and patients in high-risk group had obviously poorer OS ( $P < 0.05$ ). The ROC analysis confirmed good performance of FRGSig in all patients with different clinical characteristics (Figs. S5–8). These results suggested that the FRGSig was an independently applicable prognostic predictor.

### 3.5. Correlation between FRGSig and TMB, tumor immune infiltration

As the TMB is a critical biomarker for immune checkpoint therapy in CM patient, we analyzed the differences in somatic mutation distribution. We found that FRGSig risk score was significantly and negatively associated with TMB ( $r = -0.138$ ,  $P = 0.003$ ) (Fig. 6A), and low-risk patients exhibited more extensive TMB than high-risk patients (Fig. 6B).

Immune infiltration of tumors could be regulated by the immune checkpoints, we therefore contrasted the expression levels of ICGs in terms of risk groups. The results displayed a significant negative relationship between FRGSig risk score and the expression levels of almost all ICGs ( $P < 0.0001$ ) except CD276 (Fig. 6A). Besides, a statistically significant distinction in ICGs expression was observed between the two groups ( $P < 0.001$ ). Almost all ICGs were upregulated in the low-risk group (Fig. 6B). These results implied that the FRGSig may be involved in the immune process, and that immune checkpoint-related pathways may be play a crucial role in the favorable outcome of the low-risk patients.

### 3.6. Functional annotation and enrichment analysis

To further understand the biological functions and pathways associated with FRGSig, GO, KEGG, Reactome pathway and processes enrichment analyses with respect to different risk groups were conducted. GSEA on the TCGA CM cohort revealed that immune-related terms, including “HALLMARK IL2 STAT5 SIGNALING”, “HALLMARK INFLAMMATORY RESPONSE”, “HALLMARK INTERFERON GAMMA RESPONSE” and “HALLMARK APOPTOSIS” were differentially enriched in the low-risk patients (Fig. S9A). For KEGG pathway, “RIG I LIKE RECEPTOR SIGNALING PATHWAY”, “TOLL LIKE RECEPTOR SIGNALING PATHWAY”, “APOPTOSIS

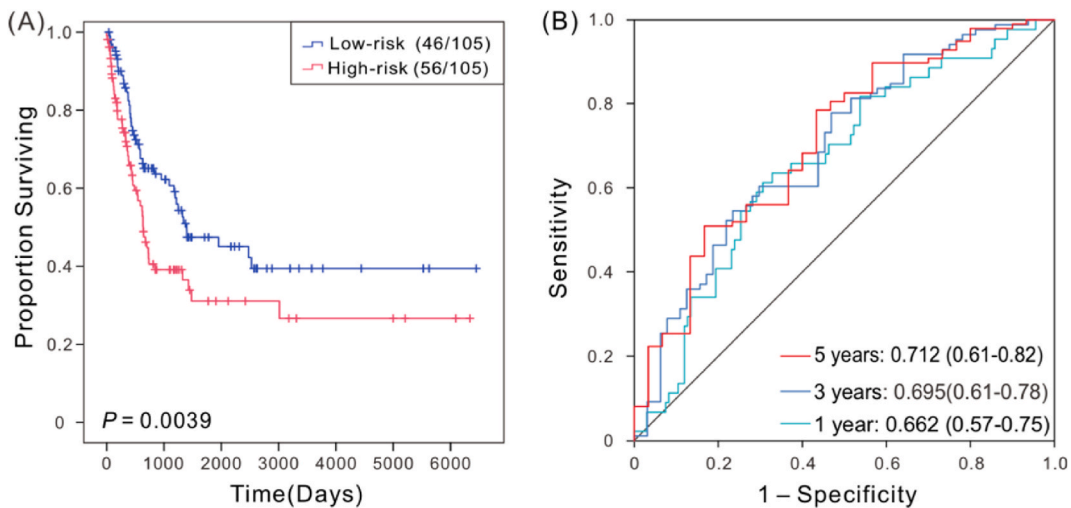


**Fig. 4. Validation of the FRGSig in independent GEO dataset. (A)** Kaplan–Meier analysis. **(B)** ROC analysis showed the sensitivity and specificity of the FRGSig in GEO cohort.

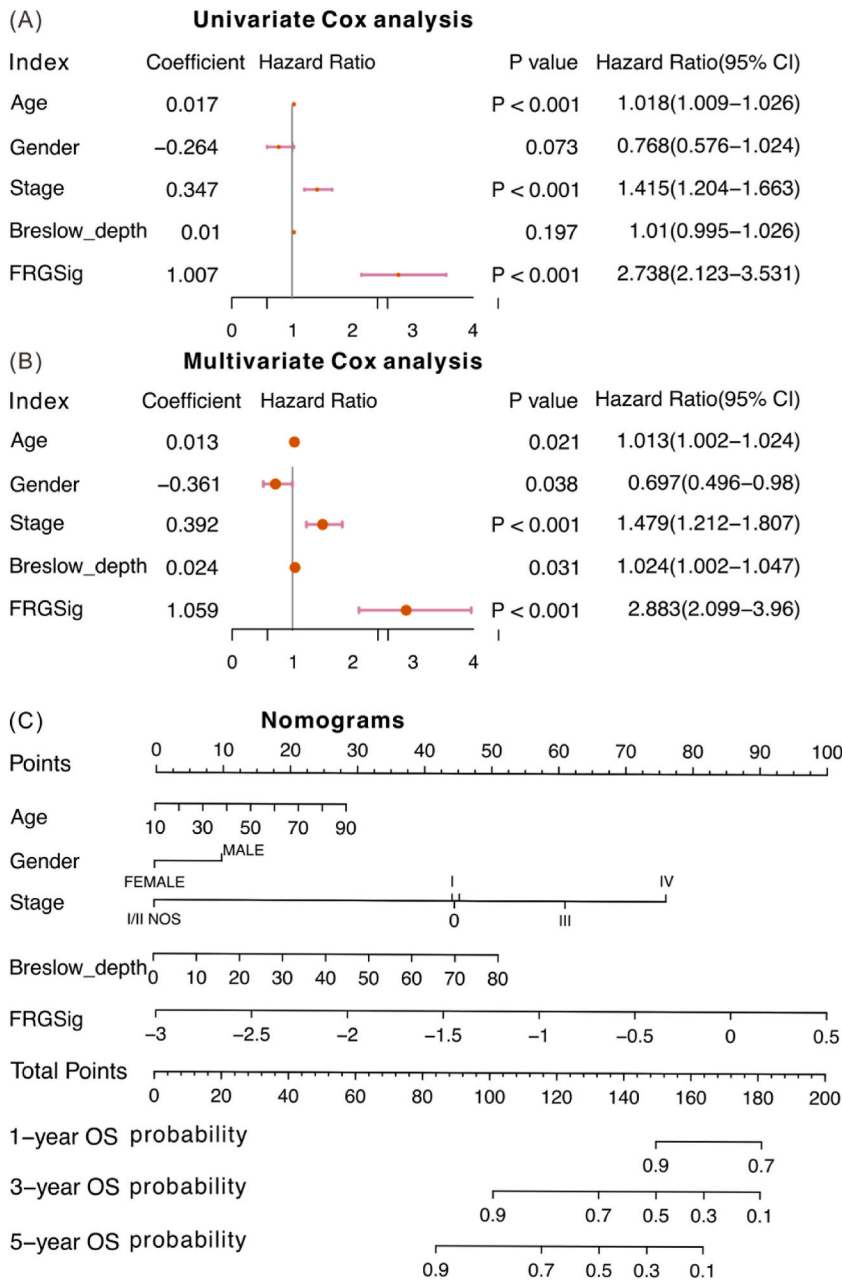


**Fig. 5. Independent prognostic factor analysis.** Forest plots showed the relationship between OS rates and clinical features in the univariate (A) and multivariate (B) Cox regression analysis. (C) Nomogram combined with FRGSig and clinicopathological variables to predicts the OS of CM patients at 1, 3, and 5 years.

PATHWAY” and “T CELL RECEPTOR SIGNALING PATHWAY” were enriched in the low-risk patients (Fig. S9B). With respect to Reactome processes, “DDX58 IFIH1 MEDIATED INDUCTION OF INTERFERON ALPHA BETA”, “REGULATED NECROSIS”, “TNF SIGNALING” and “PROGRAMMED CELL DEATH” were predominantly concentrated in the low-risk group (Fig. S9C). GO analysis showed that regulation of response to biotic stimulus, type I interferon production, hydrolase activity, peptide binding, were enriched into the low-risk group (Fig. S10). These results suggested that the FRGSig was implicated in the apoptosis and immune-related pathways.

**4. Discussion**

Ferroptosis is a recently discovered nonapoptotic cell death type. A growing body of researches have confirmed that the significant

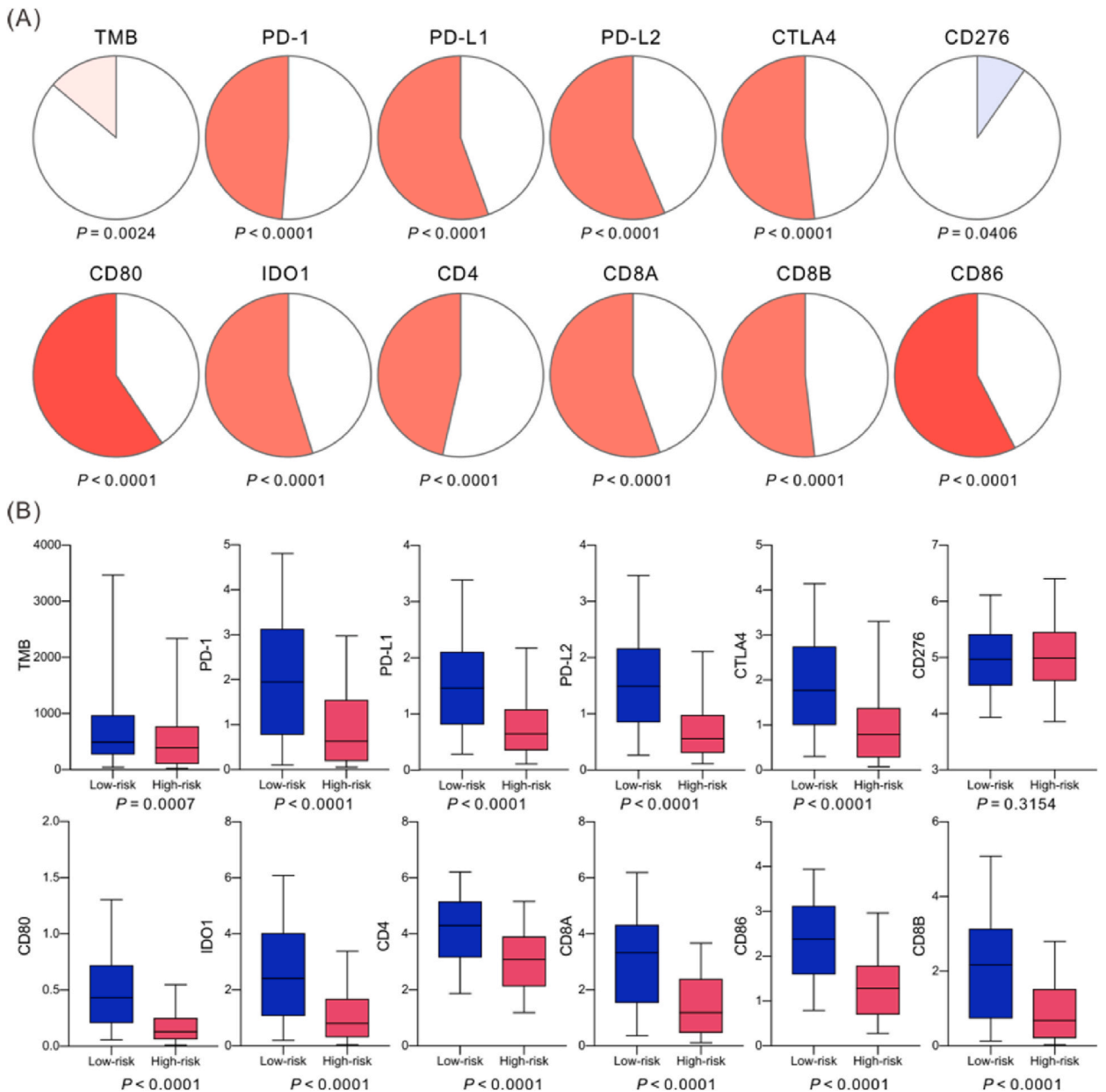


**Fig. 6.** (A) Correlation between FRGSig and TMB, ICGs. (B) The difference of TMB and expression values of ICGs between patients in high- and low-risk groups. The differences between the two groups was compared using the Mann–Whitney *U* test, and *P* values are shown under the figure.

role of ferroptosis in inducing tumor cell death and inhibiting tumor growth as well as predicting prognosis [23]. For example, the abundant expression of FRG SAT1 was linked to poor prognosis in low-grade glioma [24]; Zhang et al. found that inhibition of IRP1 (iron regulatory protein 1) expression can regulate iron homeostasis and survival of hepatocellular carcinoma cells [25]. SLC7A11 is lowly expressed, and may be used as a prognostic marker and treatment target in HPV-positive head and neck cancer [26]. However, the connection between FRGs and CM prognosis is yet to be explored. The development of novel prognostic signatures based on FRGs can be used to assess patient outcome and guide personalized treatment of CM. In this study, we comprehensively evaluated FRGs and their correlations with patient prognosis, and established a prognostic signature composed of five FRGs that could significantly distinct the OS of CM patients.

Some studies have indicated the crucial role of ferroptosis in tumor immunotherapy effectiveness [27]. Patients with higher abundance of CD8<sup>+</sup> T cells were more probably to receive benefit from immune checkpoint inhibitor therapy [28]. Neoantigens generated by somatic mutations in tumor DNA are identified and targeted by the immune system, and the more somatic mutations are produced, the more neoantigens are created [29]. Here we found that high TMB, and elevated expression of ICGs such as PD-1, PD-L1,

CD4, CD8A in patients with low FRGSig risk score. GSEA showed that IL2 STAT5 signaling pathway, inflammatory response, apoptosis pathway, TNF signaling pathway and programmed cell death pathway were predominantly enriched in the low-risk group. These results suggested that immune checkpoint-associated pathways may play a crucial function in the favorable outcome of low-risk patients and the increased antitumor immunity may be the responsible.

Ideal prognostic signature should be independent of clinical factors. In this study, we found that the FRGSig was an independent prognostic biomarker. The analysis based on the grouping of clinical characteristics indicated that regardless of gender, age, stage and tumor thickness, the FRGSig worked well in identifying low- and high-risk groups. The nomogram analysis based on the FRGSig and other clinical feature validated the satisfactory performance in the prediction of OS. Our results indicated that the FRGSig was an independently applicable prognostic biomarker with potential clinical application.

The five FRGs included in this study have been shown to be crucial in tumor development, including CM. For example, ARNTL, also known as BMAL1, is a ferroptosis suppressor by repressing the transcription of EglN2 [30]. ARNTL2 was significantly upregulated in some tumors [31–33], and knockdown of ARNTL2 suppressed the invasion and migration [31] of cancer cells. ARNTL2 was involved in immune response processes, and its high expression was positively related to activated CD4 memory T cells, and neutrophil infiltration, which can serve as a predictor for survival of patients with triple-negative breast cancer [34] and renal cell cancer [35]. However, the underlying molecular function of ARNTL in CM are not yet clear. EGFR is a validated drug target for cancer chemotherapy. It is reported that EGFR was overexpressed in various types of cancers [36–39]. Inhibition of EGFR expression had some effects on tumor-specific immune responses [40]. IFNG is a pleiotropic immunomodulatory cytokine, acts on stromal and tumor cells in an inflamed or tumor microenvironment. The expression of IFNG was a prognostic biomarker for colon cancer [41]. NOX4 has been described to be implicated in various functions such as regulation of cell proliferation, migration and death, can serve as the potential therapeutic target [42,43]. NOX4-derived ROS signaling is involved in TGF- $\beta$ -induced epithelial-mesenchymal transition [44]. TFAP2C, acting as either an oncogene or tumor suppressor, has been related to cell proliferation, tumor progression, and patient prognosis in various tumors [45–48]. Here we found these five FRGs exerted significantly different expression between cancer and normal tissues (Fig. S3). ARNTL, EGFR and TFAP2C were significantly lower expressed in CM than normal tissues, and the other two genes were significantly overexpressed in CM ( $P < 0.001$ ). IHC analysis of the normal skin tissue and tumor tissue revealed that differences expression in the remaining four genes except for the absence of NOX4. Despite the fact that the function mechanism of these five genes in CM requires supplemental basic experiments to further investigate, the significant correlation between FRGSig and the OS of CM patients and ICGs, suggested that the FRGSig might also be appropriate as biomarkers for immunotherapeutic response.

This study has several limits. It was a retrospective research in which prognostic signatures was developed based on data from publicly available databases. Although it has been validated in an independent dataset, the FRGSig requires to be further validated in clinical trials. The mechanisms of correlation between FRGs and tumor immunization in CM still warrant further investigation.

In conclusion, we established and validated a prognostic signature composed of five FRGs that proved to be independently stable and effective in anticipating the outcome of CM patients. The FRGSig was linked to TMB and tumor immune infiltration, and had potential implications for adjunctive administration and response to ICB immunotherapy in CM patients. This study provides new avenue for developing new therapeutic target and drugs innovations.

#### Author contribution statement

Wenna Guo: Conceived and designed the experiments; Wrote the paper.

Xue Wang: Performed the experiments; Analyzed and interpreted the data.

Yanting Zhang, Hongtao Liu: Performed the experiments; Analyzed and interpreted the data; Wrote the paper.

Shanshan Ma, Fangxia Guan: Contributed reagents, materials, analysis tools or data.

#### Funding statement

Wenna Guo was supported by The National Natural Science Foundation of China [No. 82103055]; China Post-Doctoral Innovative Talent Support Program [No. BX20200308]; The Key Science and Technology Research Project of Henan Province of China [No. 212102310175].

Pro. Fangxia Guan was supported by Overseas Expertise Introduction Project for Discipline Innovation [CXJD2021002].

Yanting Zhang was supported by the Natural Science Foundation of Henan Province [No. 202300410404].

#### Data availability statement

The results shown in this manuscript are based upon the data generated by the TCGA Research Network: <http://cancergenome.nih.gov/>, NCBI GEO database: <https://www.ncbi.nlm.nih.gov/geo/>, (GEPiA) database (<http://gepia.cancer-pku.cn/>), The Human Protein Atlas (<http://www.proteinatlas.org/>), FerrDb database (<http://www.zhounan.org/ferrdb/>).

#### Declaration of interests

All authors declare that they have no conflicts of interest.

## Appendix A. Supplementary data

Supplementary data to this article can be found online at <https://doi.org/10.1016/j.heliyon.2023.e15725>.

## References

- [1] O. Michielin, et al., Cutaneous melanoma: ESMO Clinical Practice Guidelines for diagnosis, treatment and follow-up, *Ann. Oncol.* 30 (12) (2019) 1884–1901.
- [2] L.E. Davis, S.C. Shalin, A.J. Tackett, Current state of melanoma diagnosis and treatment, *Cancer Biol. Ther.* 20 (11) (2019) 1366–1379.
- [3] D. Grossman, C. Sweeney, J.A. Doherty, The rapid rise in cutaneous melanoma diagnoses, *N. Engl. J. Med.* 384 (14) (2021) e54.
- [4] H. Qiu, S. Cao, R. Xu, Cancer incidence, mortality, and burden in China: a time-trend analysis and comparison with the United States and United Kingdom based on the global epidemiological data released in 2020, *Cancer Commun.* 41 (10) (2021) 1037–1048.
- [5] K.D. Miller, et al., Cancer treatment and survivorship statistics, *CA A Cancer J. Clin.* 69 (5) (2019) 363–385, 2019.
- [6] E.A.L. Enninga, et al., Survival of cutaneous melanoma based on sex, age, and stage in the United States, 1992–2011, *Cancer Med.* 6 (10) (2017) 2203–2212.
- [7] L.W. Ding, et al., LNK suppresses interferon signaling in melanoma, *Nat. Commun.* 10 (1) (2019) 2230.
- [8] R. Puglisi, et al., Biomarkers for diagnosis, prognosis and response to immunotherapy in melanoma, *Cancers* 13 (12) (2021).
- [9] Y. Cai, et al., A ferroptosis-related gene prognostic index to predict temozolomide sensitivity and immune checkpoint inhibitor response for glioma, *Front. Cell Dev. Biol.* 9 (2021), 812422.
- [10] C. Zhang, et al., Ferroptosis in cancer therapy: a novel approach to reversing drug resistance, *Mol. Cancer* 21 (1) (2022) 47.
- [11] F. Huang, et al., Ferroptosis-related gene AKRIC1 predicts the prognosis of non-small cell lung cancer, *Cancer Cell Int.* 21 (1) (2021) 567.
- [12] Z. Hu, et al., A potential mechanism of temozolomide resistance in glioma-ferroptosis, *Front. Oncol.* 10 (2020) 897.
- [13] M. Luo, et al., miR-137 regulates ferroptosis by targeting glutamine transporter SLC1A5 in melanoma, *Cell Death Differ.* 25 (8) (2018) 1457–1472.
- [14] C. International Cancer Genome, et al., International network of cancer genome projects, *Nature* 464 (7291) (2010) 993–998.
- [15] H. Cirenajwis, et al., Molecular stratification of metastatic melanoma using gene expression profiling: prediction of survival outcome and benefit from molecular targeted therapy, *Oncotarget* 6 (14) (2015) 12297–12309.
- [16] R. Cabrera, et al., Tertiary lymphoid structures improve immunotherapy and survival in melanoma, *Nature* 577 (7791) (2020) 561–565.
- [17] S. Rai, P. Mishra, U.C. Ghoshal, Survival analysis: a primer for the clinician scientists, *Indian J. Gastroenterol.* 40 (5) (2021) 541–549.
- [18] A. Barakat, et al., Understanding survival analysis: actuarial life tables and the Kaplan-Meier plot, *Br. J. Hosp. Med.* 80 (11) (2019) 642–646.
- [19] P.J. Heagerty, T. Lumley, M.S. Pepe, Time-dependent ROC curves for censored survival data and a diagnostic marker, *Biometrics* 56 (2) (2000) 337–344.
- [20] F. Ponten, et al., The Human Protein Atlas as a proteomic resource for biomarker discovery, *J. Intern. Med.* 270 (5) (2011) 428–446.
- [21] M. Lindskog, et al., Selection of protein epitopes for antibody production, *Biotechniques* 38 (5) (2005) 723–727.
- [22] A. Subramanian, et al., Gene set enrichment analysis: a knowledge-based approach for interpreting genome-wide expression profiles, *Proc. Natl. Acad. Sci. U. S. A.* 102 (43) (2005) 15545–15550.
- [23] D. Tang, et al., Ferroptosis: molecular mechanisms and health implications, *Cell Res.* 31 (2) (2021) 107–125.
- [24] Y. Mou, et al., Abundant expression of ferroptosis-related SAT1 is related to unfavorable outcome and immune cell infiltration in low-grade glioma, *BMC Cancer* 22 (1) (2022) 215.
- [25] T. Zhang, et al., ENO1 suppresses cancer cell ferroptosis by degrading the mRNA of iron regulatory protein 1, *Nat. Can. (Ott.)* 3 (1) (2022) 75–89.
- [26] A. Hemon, et al., SLC7A11 as a biomarker and therapeutic target in HPV-positive head and neck Squamous Cell Carcinoma, *Biochem. Biophys. Res. Commun.* 533 (4) (2020) 1083–1087.
- [27] Z. Li, L. Rong, Cascade reaction-mediated efficient ferroptosis synergizes with immunomodulation for high-performance cancer therapy, *Biomater. Sci.* 8 (22) (2020) 6272–6285.
- [28] J.R. Kane, et al., CD8(+) T-cell-mediated immunoeediting influences genomic evolution and immune evasion in murine gliomas, *Clin. Cancer Res.* 26 (16) (2020) 4390–4401.
- [29] T.A. Chan, et al., Development of tumor mutation burden as an immunotherapy biomarker: utility for the oncology clinic, *Ann. Oncol.* 30 (1) (2019) 44–56.
- [30] M. Yang, et al., Clockphagy is a novel selective autophagy process favoring ferroptosis, *Sci. Adv.* 5 (7) (2019) eaaw2238.
- [31] M. Lu, et al., ARNTL2 knockdown suppressed the invasion and migration of colon carcinoma: decreased SMOC2-EMT expression through inactivation of PI3K/AKT pathway, *Am. J. Trans. Res.* 12 (4) (2020) 1293–1308.
- [32] Z. Wang, et al., ARNTL2 promotes pancreatic ductal adenocarcinoma progression through TGF/BETA pathway and is regulated by miR-26a-5p, *Cell Death Dis.* 11 (8) (2020) 692.
- [33] G. Mazzoccoli, et al., ARNTL2 and SERPINE1: potential biomarkers for tumor aggressiveness in colorectal cancer, *J. Cancer Res. Clin. Oncol.* 138 (3) (2012) 501–511.
- [34] X. Wang, et al., ARNTL2 is a prognostic biomarker and correlates with immune cell infiltration in triple-negative breast cancer, *Pharmgen. Per. Med.* 14 (2021) 1425–1440.
- [35] S. Wang, et al., Upregulation of ARNTL2 is associated with poor survival and immune infiltration in clear cell renal cell carcinoma, *Cancer Cell Int.* 21 (1) (2021) 341.
- [36] C. Arienti, S. Pignatta, A. Tesei, Epidermal growth factor receptor family and its role in gastric cancer, *Front. Oncol.* 9 (2019) 1308.
- [37] J.G. Paez, et al., EGFR mutations in lung cancer: correlation with clinical response to gefitinib therapy, *Science* 304 (5676) (2004) 1497–1500.
- [38] N. Sugawa, et al., Identical splicing of aberrant epidermal growth factor receptor transcripts from amplified rearranged genes in human glioblastomas, *Proc. Natl. Acad. Sci. U. S. A.* 87 (21) (1990) 8602–8606.
- [39] C.L. Arteaga, J.A. Engelman, ERBB receptors: from oncogene discovery to basic science to mechanism-based cancer therapeutics, *Cancer Cell* 25 (3) (2014) 282–303.
- [40] F. MacDonald, D.M.W. Zaiss, The immune system's contribution to the clinical efficacy of EGFR antagonist treatment, *Front. Pharmacol.* 8 (2017) 575.
- [41] T. Yue, et al., Autophagy-related IFNG is a prognostic and immunochemotherapeutic biomarker of COAD patients, *Front. Immunol.* 14 (2023), 1064704.
- [42] Y. Bi, et al., NOX4: a potential therapeutic target for pancreatic cancer and its mechanism, *J. Transl. Med.* 19 (1) (2021) 515.
- [43] X. Wang, et al., Circular RNA NOX4 promotes the development of colorectal cancer via the microRNA4855p/CKS1B axis, *Oncol. Rep.* 44 (5) (2020) 2009–2020.
- [44] R. Hiraga, et al., Nox4-derived ROS signaling contributes to TGF-beta-induced epithelial-mesenchymal transition in pancreatic cancer cells, *Anticancer Res.* 33 (10) (2013) 4431–4438.
- [45] E. Penna, et al., microRNA-214 contributes to melanoma tumour progression through suppression of TFAP2C, *EMBO J.* 30 (10) (2011) 1990–2007.
- [46] T.H. Chang, et al., Upregulation of microRNA-137 expression by Slug promotes tumor invasion and metastasis of non-small cell lung cancer cells through suppression of TFAP2C, *Cancer Lett.* 402 (2017) 190–202.
- [47] S.L. Gao, et al., miR-200a inhibits tumor proliferation by targeting AP-2gamma in neuroblastoma cells, *Asian Pac. J. Cancer Prev. APJCP* 15 (11) (2014) 4671–4676.
- [48] C.E. Høei-Hansen, et al., Transcription factor AP-2gamma is a developmentally regulated marker of testicular carcinoma in situ and germ cell tumors, *Clin. Cancer Res.* 10 (24) (2004) 8521–8530.